Galfenol Tactile Sensor Array and Visual Mapping System

Kathleen Hale[1] Alison Flatau[2]

ABSTRACT

The smart material, Galfenol, is being explored for its uses as a magnetostrictive material. This project seeks to determine if Galfenol can be used as a tactile sensor in a 2-D grid array, magnetic circuit system. When used within a magnetic circuit, Galfenol indicates induced stress and force as a change in flux, due to a change in permeability of the material. The change in flux is detected by Giant MagnetoResistive (GMR) Sensors, which produce a voltage change proportional to the field change. By using Galfenol in an array, this research attempts to create a sensory area.

Galfenol is an alloy made of Iron and Gallium. Fe_xGa_x, where $15 \leq x \leq 28$, creates a material with useful mechanical and transduction attributes (Clark et al and Kell). Galfenol is also distinguished by the crystalline structure of the material. Two types currently exist: single crystal and polycrystalline. Single crystal has higher transduction coefficients than polycrystalline, but is more costly. Polycrystalline Galfenol is currently available as either production or research grade. The designations are related to the sample growth rate with the slower rate being the research grade. The slower growth rate more closely resembles the single crystal Galfenol properties. Galfenol 17.5- 18% research grade is used for this experiment, provided by Etrema Products Inc.

The magnetic circuit and sensor array is first built at the macro scale so that the design can be verified. After the macro scale is proven, further development will move the system to the nano-level. Recent advances in nanofabrication have enabled Galfenol to be grown as nanowires. Using the nanowires, research will seek to create high resolution tactile sensors with spatial resolutions similar to human finger tips, but with greater force ranges and sensitivity capabilities (Flatau & Stadler). Possible uses of such systems include robotics and prosthetics.

CIRCUIT DESIGN

Nine Galfenol rods of 1/8" diameter by ¼" long are arranged in a 3x3 grid array. The rods are evenly spaced with 3/16" distance between rod centers. A grade 1 ceramic magnet sits below the rods which produces the flux through the system. The magnetic circuit is completed by 1010 steel pathways. At the top of the rods the steel is separated by small gaps to encourage the flux to travel along paths indicative of the rod it covers (See Figure 1). Magnetic flux travels the shortest path back to the magnet and along the path of greatest permeability. Therefore

[1] NASA Goddard Space Flight Center and University of Maryland, College Park
[2] University of Maryland, College Park

the flux is directed certain ways as steel has a higher relative permeability, μ=1156, than air, μ=1. The flux from the magnet travels up through the Galfenol rods, through the 1010 steel paths, and then to the sides of the circuit where the GMR sensors are located. Next, the flux travels down the side wall steel paths to a bottom layer of steel which the magnet rests upon, closing the circuit.

The steel pathways on the sides of the circuit are separated by Aluminum spacers. The size of the spacers can be varied for investigation into the effect of separation distance between the steel paths on the flux flow.

The layer of steel at the top of the Galfenol rods is a group of steel pieces, placed together to create pathways to the sides. This steel layer is sectioned in order to allow force to be applied to one rod at a time without affecting the others.

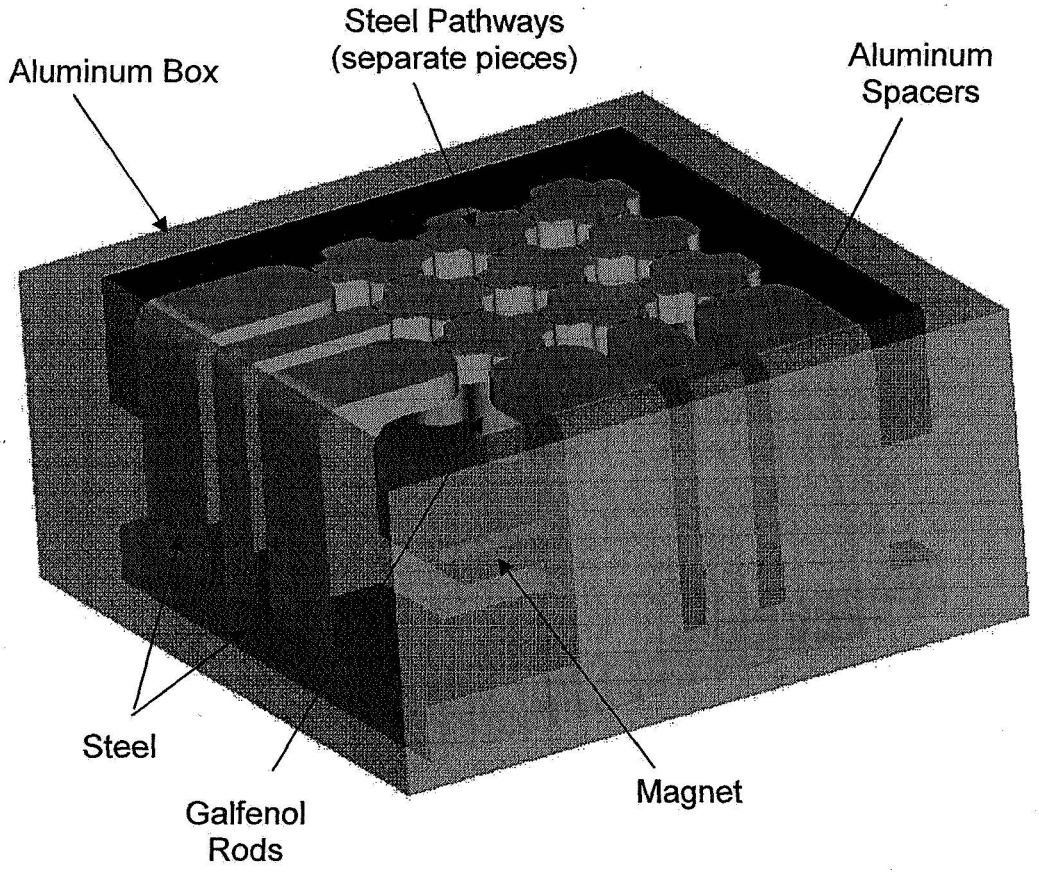

Figure 1. Circuit Design

CIRCUIT OPTIMIZATION

Magnetic modeling is performed to optimize the circuit design for efficiency and for determining the best location for the GMR sensors. Two software programs are used; Oersted (2-Dimensional) and Amperes (3-Dimensional). Initial modeling is performed using Oersted, and more accurate analysis is completed using Amperes. Oersted simplifies the circuit by assuming a constant design through a user specified depth. Figure 2 shows a 2-D model of 2 Galfenol rods under no stress on top of a grade 1 ceramic magnet. Galfenol material info aquired from "Atulasimha" reference.

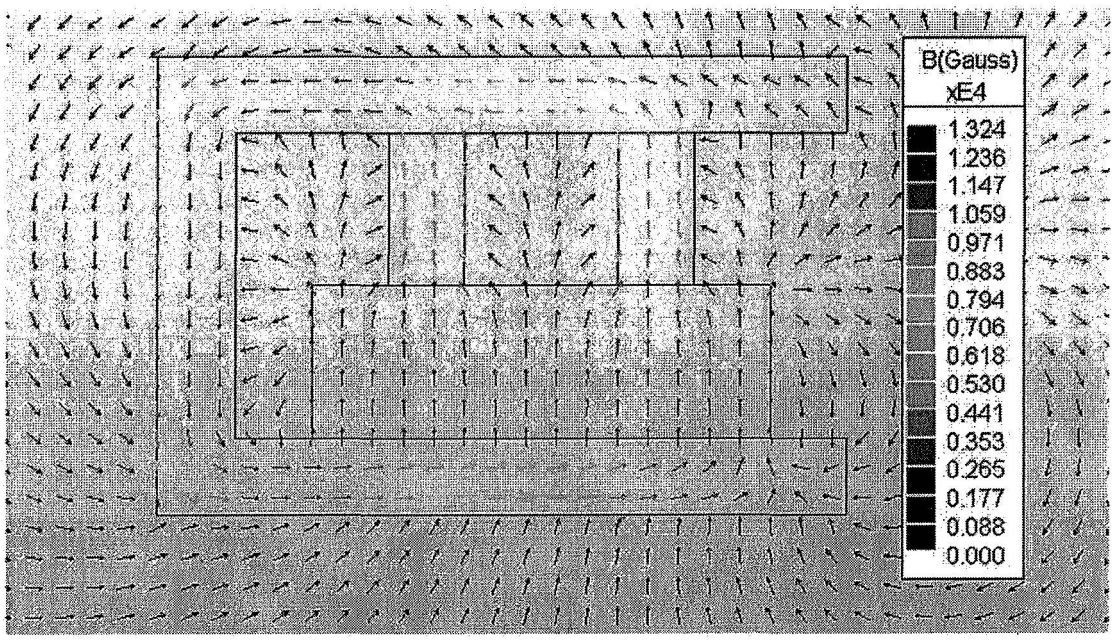

Figure 2. 2-D Models of the Magnetic Circuit Design

The analysis allows determination of where the maximum flux level occurs and therefore where the GMR sensor should be located.

Once the basic circuit design is chosen, a more detailed analysis is performed using Amperes. The following figures depict Amperes 3-D analyses results. Information on how the B-H curve of the Galfenol material changes due to applied stress is used in the model to investigate how the flux level changes at different locations when force is applied to one rod in the array. Figure 3 depicts the flux density in one row of Galfenol rods when the array is in the nominal, no stress configuration. The greatest concentration of flux is shown to be along the top level of steel near the left side. This information contributes to the decision to locate the GMR sensor close to this location. Figure 4 shows the flux density along the top steel pathways with no rods under stress.

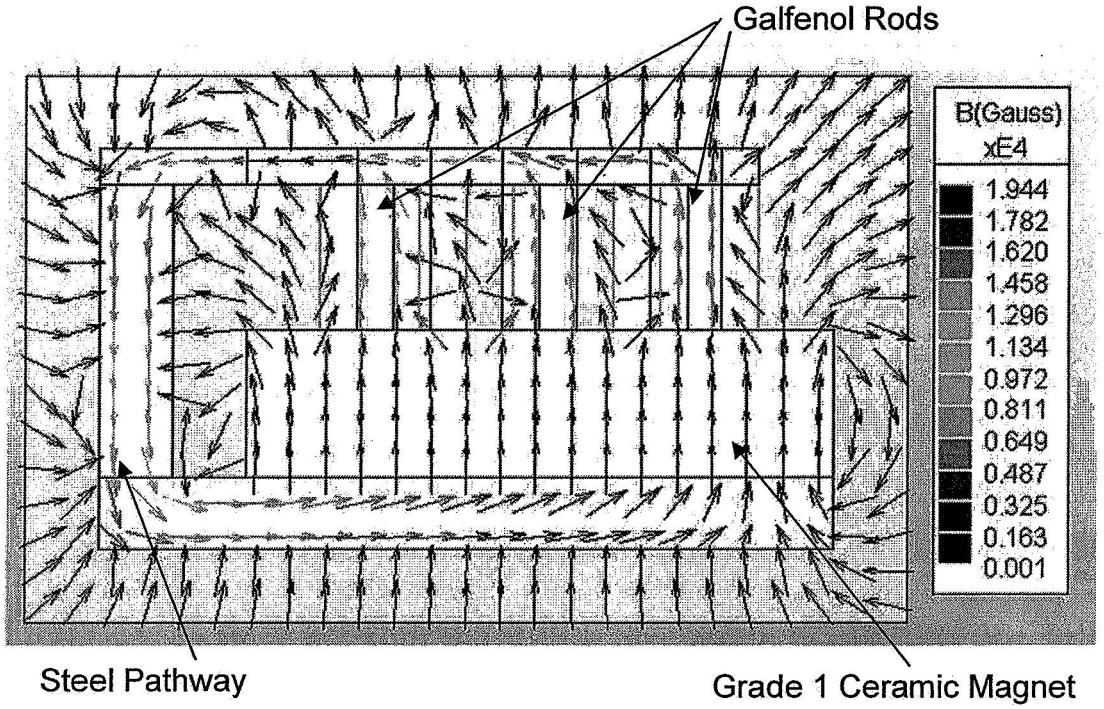

Figure 3. Side view of Galfenol rods under no stress

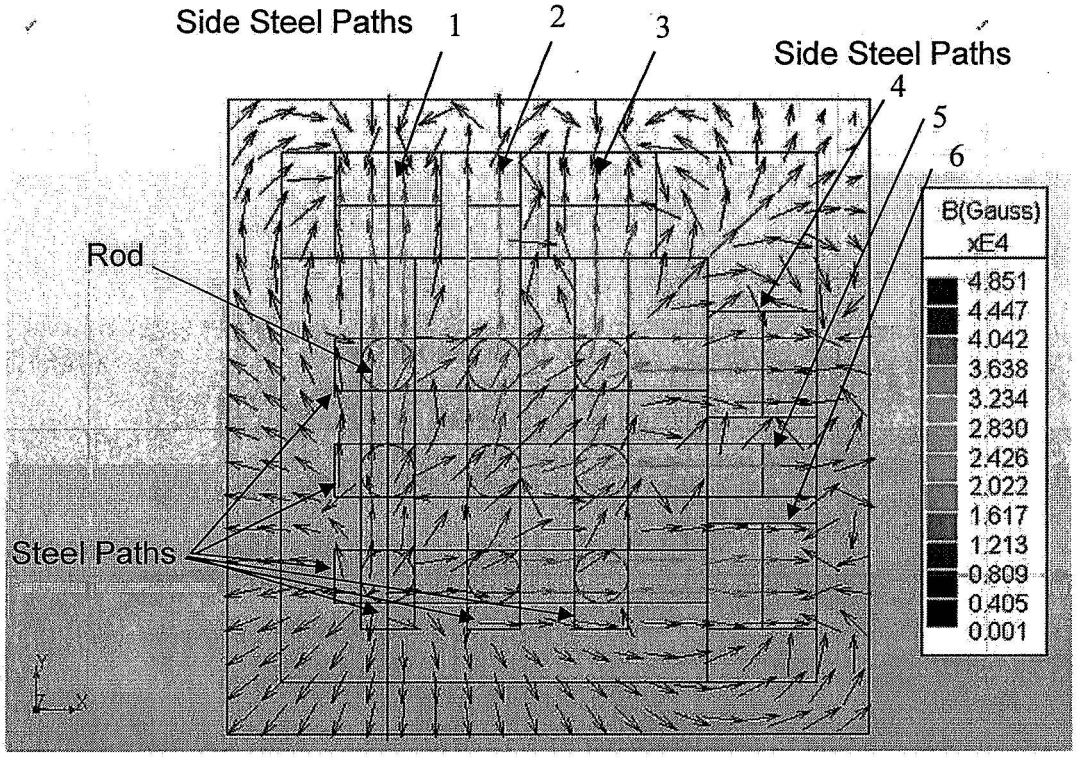

Figure 4. Top view of flux pathway along top of Galfenol rod array. No rods are under stress.

The following Figure 5 shows the flux density change when the central rod is stressed by a 15 MPa.

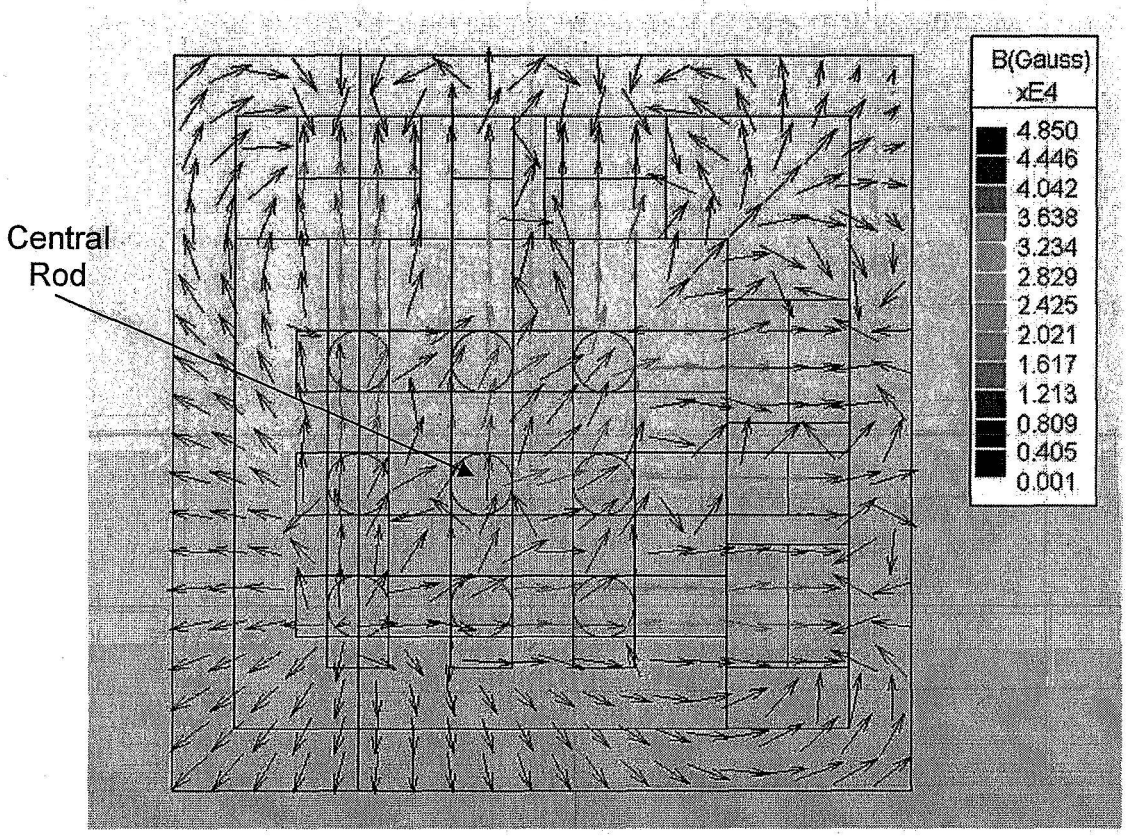

Figure 5. Central rod stressed at 15 MPa

Though it is not obvious by the figures, values shown in the following chart are taken from the models and compared. From these values, it is shown that the largest change in flux is indeed at the two side paths which intersect at the rod that is stressed. In this case, when 15MPa of stress is applied to Side Steel Paths #2 and #5 change by 5 Gauss whereas the other side paths change by no more than 3 Gauss.

Table 1. Flux Density Values For Central Rod and Side Steel Paths

Location	Stress (MPa)	x(in)	y (in)	z (in)	Bm (Gauss)
Top of Central Rod	0	0.500	0.500	0.625	5651
Side Steel Path #1	0	0.250	1.125	0.688	379
Side Steel Path #2	0	0.500	1.125	0.688	636
Side Steel Path #3	0	0.750	1.125	0.688	295
Side Steel Path #4	0	1.125	0.75	0.6875	276
Side Steel Path #5	0	1.125	0.500	0.688	501
Side Steel Path #6	0	1.125	0.25	0.6875	340
Top of central rod	15	0.500	0.500	0.625	9013
Side Steel Path #1	15	0.250	1.125	0.688	382
Side Steel Path #2	15	0.500	1.125	0.688	641
Side Steel Path #3	15	0.750	1.125	0.688	296
Side Steel Path #4	15	1.125	0.75	0.6875	273
Side Steel Path #5	15	1.125	0.500	0.688	496
Side Steel Path #6	15	1.125	0.25	0.6875	338

DATA ACQUISITION

Six GMR sensors are placed along the outer perimeter of the circuit, one for each row or column of the steel pathways (See Figures 6 & 7). GMR type NVE AA-005-02 is used and has a linear range of 10 to 70 Oersteds. The sensor is excited using a voltage of 3.33V, and the signal is amplified by setting the gain to 10. This excitation and amplification is provided using the National Instruments SCXI-1121 module, -1321 terminal block and PCI-MIO-16XE data acquisition card. Labview is then used to record and view the change in flux detected during testing. One hundred samples are taken and averaged to produce one flux level reading. The samples are filtered with a 4 Hz filter.

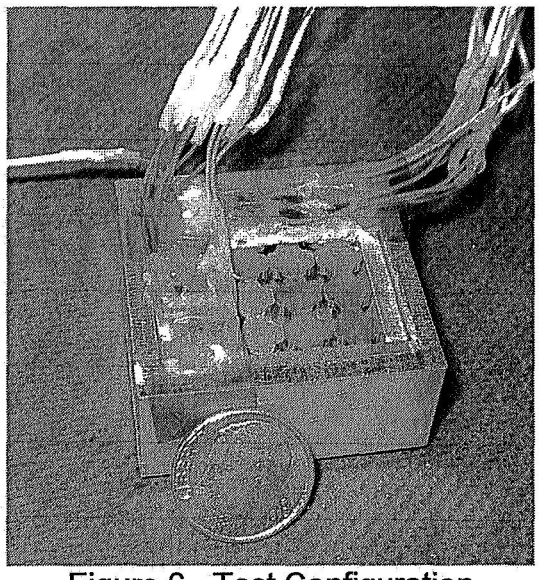

Figure 6. Test Configuration

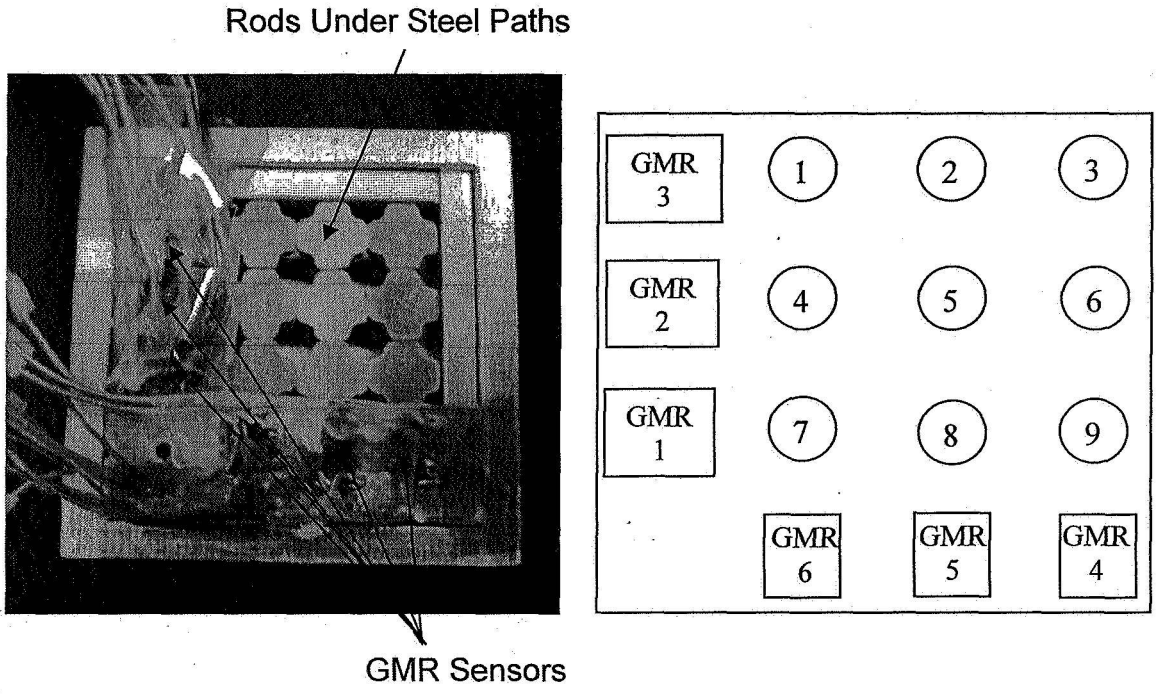

Figure 7a. Top View Photo of Circuit. Figure 7b. Representation of Rod and GMR Sensor Numbering in Magnetic Circuit

A force gage is used to apply and measure the force applied to the rods. 3.5 lb and 7.5 lb of force are applied to each rod and the GMR readings are recorded for each.

RESULTS

Tables 2 and 3 below, list the change in flux for each rod for the static 3.5 lb and 7 lb force applications, respectively. The raw data collected can be found in Appendix A. Since the GMR sensors are slightly raised above the steel pathways on the boards they are mounted to, the flux reading in Oersted is equal to the flux density in Gauss. Tables 2 and 3 also list the rod that the value changes indicate, and whether or not the indication is correct.

Table 2. Flux Change Recorded By GMR Sensors Under 3.5 lb Load

Rod	Force (lb)	GMR 1 (Oe)	GMR 2 (Oe)	GMR 3 (Oe)	GMR 4 (Oe)	GMR 5 (Oe)	GMR 6 (Oe)	Indicates Rod #	Correct *
1	3.672	-0.260	0.490	1.102	0.690	0.218	0.121	3	
2	3.662	0.030	-0.024	-0.212	-0.200	-0.097	-0.079	3	
3	3.681	-0.103	0.260	0.212	0.823	0.127	0.133	6	
4	3.684	2.767	4.057	0.618	3.021	0.036	2.016	6	
5	3.666	0.884	1.514	0.527	1.974	0.194	0.624	6	
6	3.701	0.484	-0.769	-0.006	-0.133	0.672	-0.006	5	
7	3.75	0.212	0.291	0.036	-0.817	0.539	1.447	4	
8	3.769	0.254	0.842	0.890	1.017	1.405	1.271	2	
9	3.672	-0.557	0.890	1.320	1.441	0.902	0.545	3	
1	3.662	0.109	0.872	1.556	0.993	0.763	0.624	3	
2	3.651	2.313	0.648	0.775	0.448	0.569	0.466	5	
3	3.664	0.448	0.236	0.042	-0.024	0.236	0.333	7	
4	3.648	0.787	4.105	0.539	3.639	0.048	2.168	6	
5	3.655	0.357	1.695	0.448	1.871	-0.061	0.745	6	
6	3.673	0.690	0.176	-0.206	1.308	-0.030	-0.109	9	
7	3.772	0.242	-0.218	-0.375	0.521	-0.460	3.257	1	
8	3.78	0.872	0.109	0.400	-0.666	0.975	0.896	8	*
9	3.67	-1.066	0.551	0.660	-0.672	-0.224	0.533	9	*

Table 3. Flux Change Recorded By GMR Sensors Under 7.0 lb Load

Rod	Force (lb)	GMR 1 (Oe)	GMR 2 (Oe)	GMR 3 (Oe)	GMR 4 (Oe)	GMR 5 (Oe)	GMR 6 (Oe)	Indicates Rod #	Correct *
1	7.01	1.816	0.079	0.194	0.448	-0.200	-0.218	9	
2	7.102	-1.120	0.279	0.109	0.745	-0.200	-0.200	9	
3	7.05	-0.412	0.279	1.096	1.919	0.036	0.212	3	*
4	7.025	2.961	8.676	0.545	8.180	-1.514	5.213	6	
5	7.022	-0.333	1.320	0.073	0.872	-0.557	0.642	6	
6	7.071	-0.866	-0.236	-0.327	4.559	-0.133	-1.193	9	
7	7.14	0.206	0.387	-0.194	2.755	-0.133	8.737	4	
8	7.129	0.890	0.745	0.478	2.313	0.854	5.025	7	
9	7.042	0.472	0.763	1.235	0.345	0.581	1.102	1	
1	7.047	1.241	0.624	2.737	1.865	0.200	0.406	3	
2	7.04	3.463	0.515	0.412	0.327	0.503	0.472	8	
3	7.056	0.636	0.291	0.394	1.090	0.254	0.254	9	
4	7.043	2.712	7.895	1.259	5.715	-0.551	4.172	6	
5	7.06	2.949	2.385	1.162	2.961	0.115	1.120	9	
6	7.087	0.727	1.344	0.612	3.736	0.969	1.623	6	*
7	7.139	0.484	1.187	0.418	0.006	0.575	4.795	4	
8	7.135	-0.527	-0.230	0.896	0.351	5.322	-5.316	2	
9	7.064	1.992	1.744	1.574	-0.472	1.495	2.712	7	

As shown in the results above, only 2 rods were correctly identified as having the force applied to them for both levels of load.

Figures 8 and 9 below depict the dynamic loading results for rods 4 and 7 in a 2 x 2 grid array. The figures show that rod 4 is correctly identified by the sensors that show the greatest frequency and amplitude of change during the loading. The sensor information for rod 7, however is not as obvious which may be due to

the fact that GMR 2 is located closer to the rods than GMR 1. The sensors were staggered to allow space for soldering.

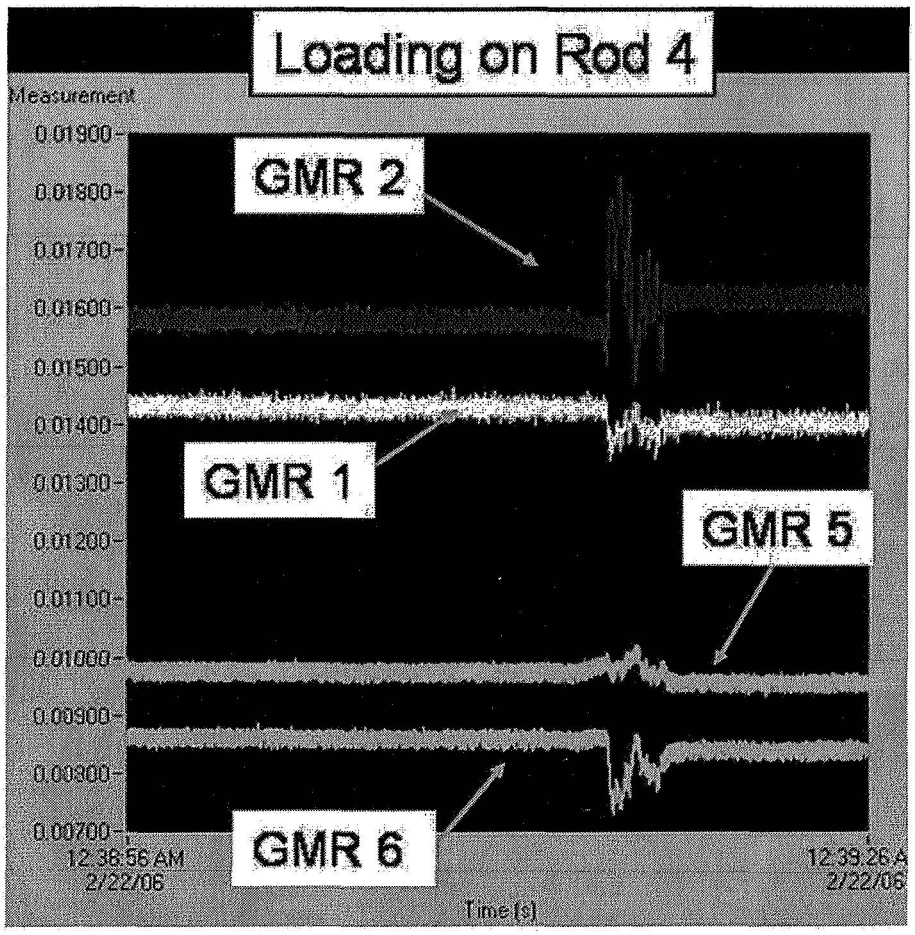

Figure 8. Dynamic Loading on Rod 4

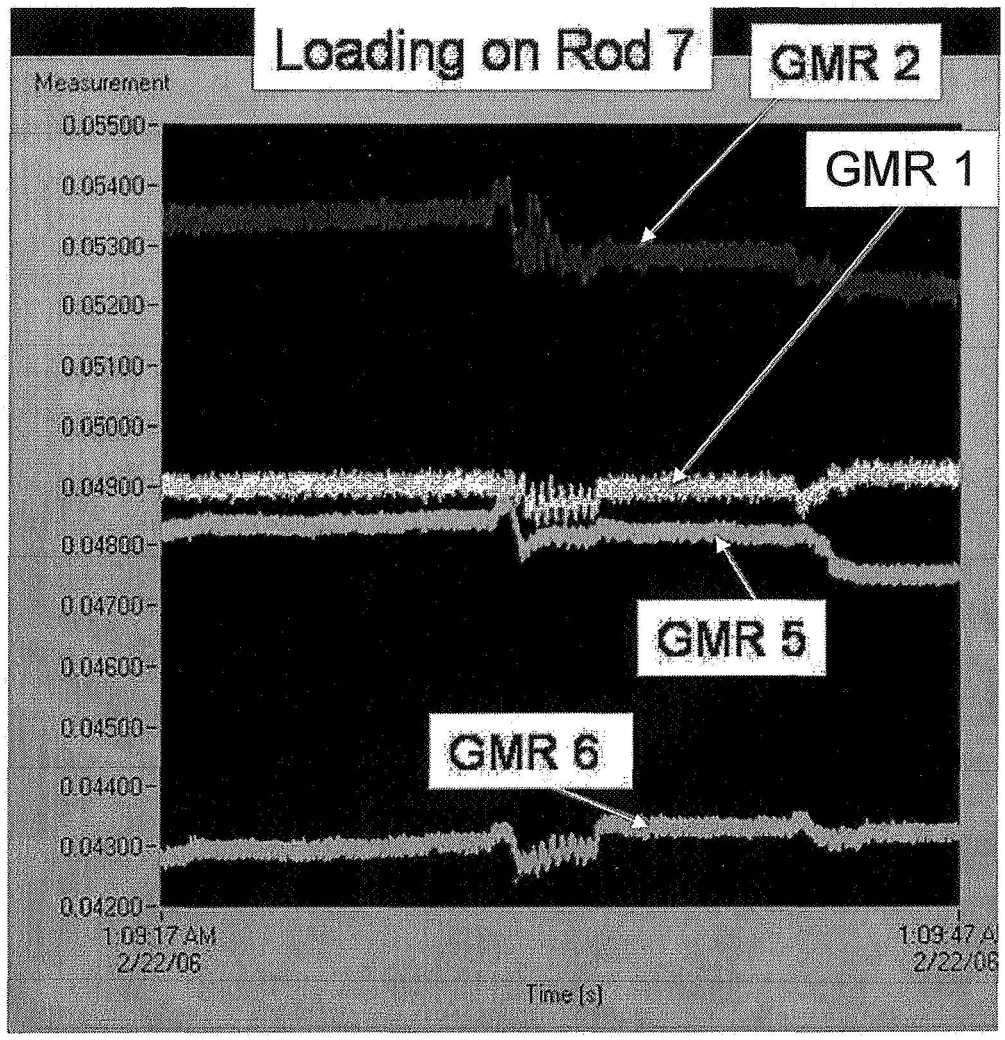

Figure 9. Dynamic Loading on Rod 7

Figure 10 below shows results for dynamic loading on rod 1 in a 3 x 3 rod array. GMRs 3 and 6 should give the greatest signal response, however, it is not completely apparent from the data collected that this is the case.

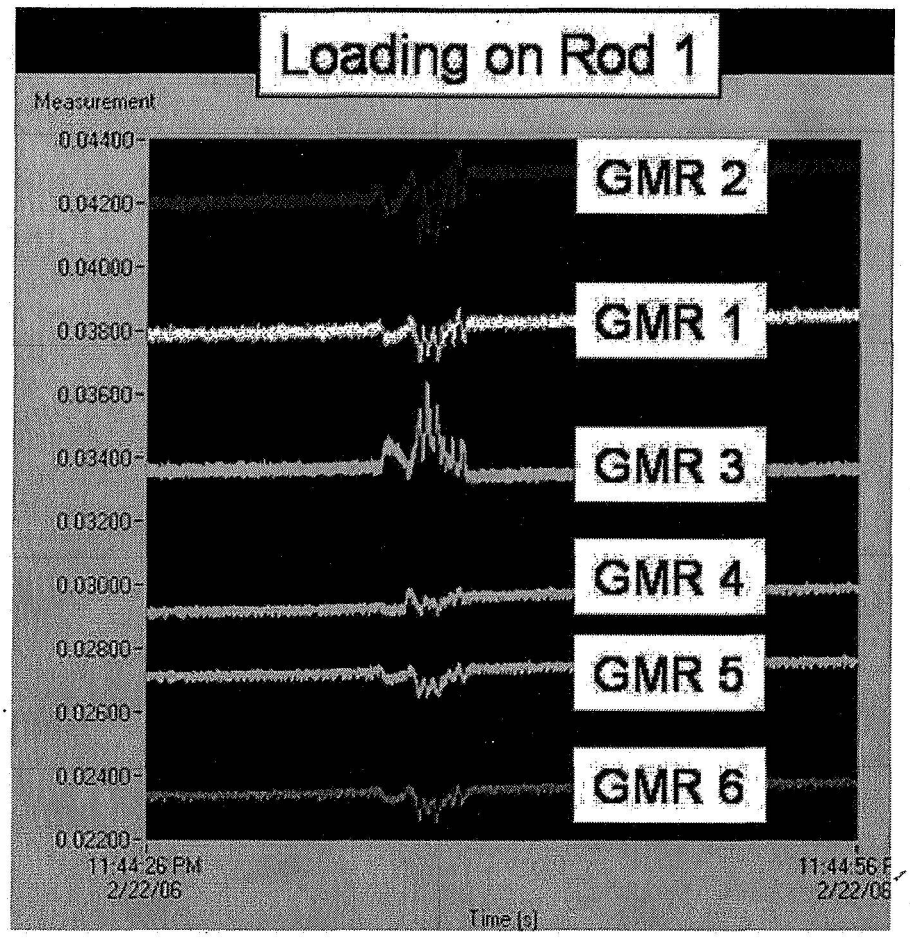

CONCLUSIONS

The initial set of static data is not very conclusive. Only 2 rods are correctly identified in each loading data set. One possible cause of error is that the noise levels may be too high and may require more samples to be averaged together to produce a more accurate result. Due to the fact that the flux change is so small, error is also possible in that the GMR sensor's sensitivity ranges from ±0.1 mV/Oe. This small difference could alter which rod has the greatest flux change. A possible solution is to increase the magnetic flux so that the change in flux for each level of force is greater, thereby making the noise level a smaller percentage of the value. However, the Amperes 3-D models show that the steel pathways are almost at saturation just before the flux reaches the sensors. Saturation for 1010 steel is about 2.25 Tesla. Therefore, if the magnetic flux is increased, the thickness of the steel should be increased to allow more flux flow to the sensors.

Dynamic loading had more accurate results. The 2x2 grid array correctly identified 3 out of 4 of the rods. The 3x3 grid array was more complex, however, and more sensitive to small differences in GMR location and flux path congruity.

AREAS FOR IMPROVEMENT

Size and proximity of GMR sensors

A definite difference was noted in the signal reaction for the dynamic loading due to how close the GMR sensor was to the rods, relative to the others. GMR 2 in this experiment consistently had a greater signal reaction due to it being positioned closer to the rods than GMRs 1 and 3. This will be changed or accounted for in future testing.

The GMR sensors used in the magnetic circuit have widths close to that of the steel pathways around the outer edges of the system. Due to the fact that the sensors and pathways were located about 1/16" from one another, questions arise as to whether or not the magnetic field one sensor is detecting is affected by the path next to it. A possible improvement would be to insert the GMR sensor into the steel path so that the flux flow goes directly through it, rather than the sensor being located over the flux flow. This may decrease the amount of proximity effect between the sensors.

The size of the sensor also raises issues when considering the future intent to create a nano-sized system. A GMR "violin" sensor exists that might be able to be incorporated to allow measurement to occur from a certain distance away from the magnetic field pathway. This would allow magnetic field pathways to be located closer together and would allow space for more of the pathways.

Congruity of flux paths

The steel paths on the tops of the rods are fabricated as separate pieces to allow force to be applied to one rod without applying force to another. However, during the experiment, gaps were created between the flux paths during loading. A magnetic grease (grease with iron filings) will be inserted between the flux path tops to allow flow to continue between them during loading.

Proximity of force gage tip

It is noted that the proximity of the force gage tip to a GMR sensor affects the flux reading. This flux offset, however, does not affect the data recorded due to the fact that an initial flux reading was recorded with the tip just above the rod (applying no force) and then this value was subtracted from the flux value when the force was applied.

FUTURE WORK

Strain gages will be placed on every rod. The strain gages collect strain information that contributes to the characterization of the Galfenol material.

The GMR sensors shall be used to not only to locate the where the force is applied, but also to determine the amount of force applied. Mathematical analysis shall be perfomed and sense coils will be placed around each rod to

record the flux change in the Galfenol rod that is being stressed. This will verify the force value determined by the GMR sensors.

SUMMARY

According to the modeling performed, the concept of using Galfenol in a grid array to determine force location is possible. This first run-through of tests has produced some success and has identified areas that need modification. By reducing noise and the effects of sensor resolution sensitivity and proximity the flux data collected will be more accurate. With the data collected here, and the future work planned, nano-sized Galfenol sensor arrays are feasible.

REFERENCES

Atulasimha, Jayasimha, and Alison Flatau. "Quasistatic Actuation Characteristics of Varied Stoichiometry Single Crystal Iron-Gallium." Department of Aerospace Engineering, University of Maryland, College Park, MD.

Flatau, Alison, and Bethanie Stadler. "Development of Nanostructured Galfenol Tactile Sensors." White paper submitted to DAPRA-DSO, 2005.

Clark et al & Kellog - will add refrence info

APPENDIX A

Data collected for 3.5 lb force:

Sample	Rod	Force (lb)	GMR 1 (V)	GMR 2 (V)	GMR 3 (V)	GMR 4 (V)	GMR 5 (V)	GMR 6 (V)
1	1	0	-0.005701	-0.000444	0.000914	-0.00253	-0.001506	-0.00019
2	1	3.672	-0.005744	-0.000363	0.001096	-0.002416	-0.00147	-0.00017
3	2	0	-0.005661	-0.00078	0.000038	-0.002474	-0.001417	-0.000157
4	2	3.662	-0.005656	-0.000784	0.000003	-0.002507	-0.001433	-0.00017
5	3	0	-0.005574	-0.00078	-0.000044	-0.002466	-0.001391	-0.000153
6	3	3.681	-0.005591	-0.000737	-0.000009	-0.00233	-0.00137	-0.000131
7	4	0	-0.005313	0.000817	0.000435	-0.002202	-0.001258	0.000395
8	4	3.684	-0.004856	0.001487	0.000537	-0.001703	-0.001252	0.000728
9	5	0	-0.005552	-0.000206	0.000313	-0.00221	-0.001083	0.000387
10	5	3.666	-0.005406	0.000044	0.0004	-0.001884	-0.001051	0.00049
11	6	0	-0.005528	-0.000094	0.000479	-0.001933	-0.000961	0.000449
12	6	3.701	-0.005448	-0.000221	0.000478	-0.001955	-0.00085	0.000448
13	7	0	-0.004326	0.000455	0.000788	-0.001741	-0.000495	0.002207
14	7	3.75	-0.004291	0.000503	0.000794	-0.001876	-0.000406	0.002446
15	8	0	-0.00483	0.000452	0.001104	-0.00229	0.000124	0.001376
16	8	3.769	-0.004788	0.000591	0.001251	-0.002122	0.000356	0.001586
17	9	0	-0.004756	0.000653	0.001353	-0.003452	0.00004	0.001253
18	9	3.672	-0.004848	0.0008	0.001571	-0.003214	0.000189	0.001343
19	9	0	-0.004403	0.000961	0.001666	-0.003002	0.000334	0.001529
20	1	0	-0.00478	0.001494	0.002841	-0.000378	0.000306	0.001569
21	1	3.662	-0.004762	0.001638	0.003098	-0.000214	0.000432	0.001672
22	2	0	-0.004359	0.001289	0.002106	-0.000214	0.000533	0.001743
23	2	3.651	-0.003977	0.001396	0.002234	-0.00014	0.000627	0.00182
24	3	0	-0.003823	0.001405	0.002119	-0.000107	0.000714	0.001911
25	3	3.664	-0.003749	0.001444	0.002126	-0.000111	0.000753	0.001966
26	4	0	-0.003359	0.002767	0.002565	-0.000145	0.000851	0.002293
27	4	3.648	-0.003229	0.003445	0.002654	0.000456	0.000859	0.002651
28	5	0	-0.003644	0.001846	0.002395	-0.000038	0.000969	0.002295
29	5	3.655	-0.003585	0.002126	0.002469	0.000271	0.000959	0.002418
30	6	0	-0.003896	0.001776	0.002394	-0.000023	0.001001	0.002256
31	6	3.673	-0.003782	0.001805	0.00236	0.000193	0.000996	0.002238
32	7	0	-0.002905	0.002166	0.002499	0.000127	0.001219	0.003829
33	7	3.772	-0.002865	0.00213	0.002437	0.000213	0.001143	0.004367
34	8	0	-0.004113	0.001795	0.002409	-0.000762	0.001438	0.002617
35	8	3.78	-0.003969	0.001813	0.002475	-0.000872	0.001599	0.002765
36	9	0	-0.00388	0.001714	0.00244	-0.002958	0.001164	0.002239
37	9	3.67	-0.004056	0.001805	0.002549	-0.003069	0.001127	0.002327
38	9	0	-0.004115	0.001778	0.00251	-0.002823	0.001143	0.002338

Data collected for 7.0 lb force:

Sample	Rod	Force (lb)	GMR 1 (V)	GMR 2 (V)	GMR 3 (V)	GMR 4 (V)	GMR 5 (V)	GMR 6 (V)
1	1	0	-0.013531	-0.008006	-0.006112	-0.009975	-0.008514	-0.007647
2	1	7.01	-0.013231	-0.007993	-0.00608	-0.009901	-0.008547	-0.007683
3	2	0	-0.013534	-0.00834	-0.007151	-0.010164	-0.008555	-0.007738
4	2	7.102	-0.013719	-0.008294	-0.007133	-0.010041	-0.008588	-0.007771
5	3	0	-0.013957	-0.008349	-0.007256	-0.010195	-0.008562	-0.007759
6	3	7.05	-0.014025	-0.008303	-0.007075	-0.009878	-0.008556	-0.007724
7	4	0	-0.013626	-0.007393	-0.006919	-0.010267	-0.00846	-0.007398
8	4	7.025	-0.013137	-0.00596	-0.006829	-0.008916	-0.00871	-0.006537
9	5	0	-0.013922	-0.007571	-0.007064	-0.009633	-0.008564	-0.007159
10	5	7.022	-0.013977	-0.007353	-0.007052	-0.009489	-0.008656	-0.007053
11	6	0	-0.014273	-0.008069	-0.007003	-0.010385	-0.008302	-0.007502
12	6	7.071	-0.014416	-0.008108	-0.007057	-0.009632	-0.008324	-0.007699
13	7	0	-0.012985	-0.007635	-0.006715	-0.00992	-0.007848	-0.005779
14	7	7.14	-0.012951	-0.007571	-0.006747	-0.009465	-0.00787	-0.004336
15	8	0	-0.013288	-0.007309	-0.006247	-0.010294	-0.007076	-0.006356
16	8	7.129	-0.013141	-0.007186	-0.006168	-0.009912	-0.006935	-0.005526
17	9	0	-0.01335	-0.007084	-0.005997	-0.01224	-0.007109	-0.006427
18	9	7.042	-0.013272	-0.006958	-0.005793	-0.012183	-0.007013	-0.006245
19	9	0	-0.013034	-0.00688	-0.005744	-0.01182	-0.006875	-0.006047
20	1	0	-0.01322	-0.006299	-0.004361	-0.008186	-0.006741	-0.005833
21	1	7.047	-0.013015	-0.006196	-0.003909	-0.007878	-0.006708	-0.005766
22	2	0	-0.01296	-0.006386	-0.005119	-0.008079	-0.006592	-0.005697
23	2	7.04	-0.012388	-0.006301	-0.005051	-0.008025	-0.006509	-0.005619
24	3	0	-0.012191	-0.006154	-0.005079	-0.008021	-0.006312	-0.005438
25	3	7.056	-0.012086	-0.006106	-0.005014	-0.007841	-0.00627	-0.005396
26	4	0	-0.011479	-0.00488	-0.00452	-0.007849	-0.006071	-0.004975
27	4	7.043	-0.011031	-0.003576	-0.004312	-0.006905	-0.006162	-0.004286
28	5	0	-0.011156	-0.004973	-0.004449	-0.007097	-0.005853	-0.004344
29	5	7.06	-0.010669	-0.004579	-0.004257	-0.006608	-0.005834	-0.004159
30	6	0	-0.010599	-0.004807	-0.004122	-0.00681	-0.005562	-0.00416
31	6	7.087	-0.010479	-0.004585	-0.004021	-0.006193	-0.005402	-0.003892
32	7	0	-0.009457	-0.004072	-0.003731	-0.006291	-0.005021	-0.002183
33	7	7.139	-0.009377	-0.003876	-0.003662	-0.00629	-0.004926	-0.001391
34	8	0	-0.009831	-0.004071	-0.003486	-0.006688	-0.004284	-0.002995
35	8	6.53	-0.009189	-0.003851	-0.003444	-0.005937	-0.004625	-0.001523
36	8	0	-0.009028	-0.003723	-0.00325	-0.005744	-0.0045	-0.001614
37	8	7.135	-0.009115	-0.003761	-0.003102	-0.005686	-0.003621	-0.002492
38	9	0	-0.008967	-0.003719	-0.002942	-0.008193	-0.004189	-0.003134
39	9	7.064	-0.008638	-0.003431	-0.002682	-0.008271	-0.003942	-0.002686
40	9	0	-0.008482	-0.003264	-0.002542	-0.007995	-0.003797	-0.00244

Galfenol Tactile Sensor Array and Visual Mapping System

Kate Hale, Alison Flatau

NASA Goddard Space Flight Center and
University of Maryland, College Park

Objective

To design a grid array of the smart material, Galfenol, in a magnetic circuit that can be used as a sensor system to relay force and force location information

Visual Mapping

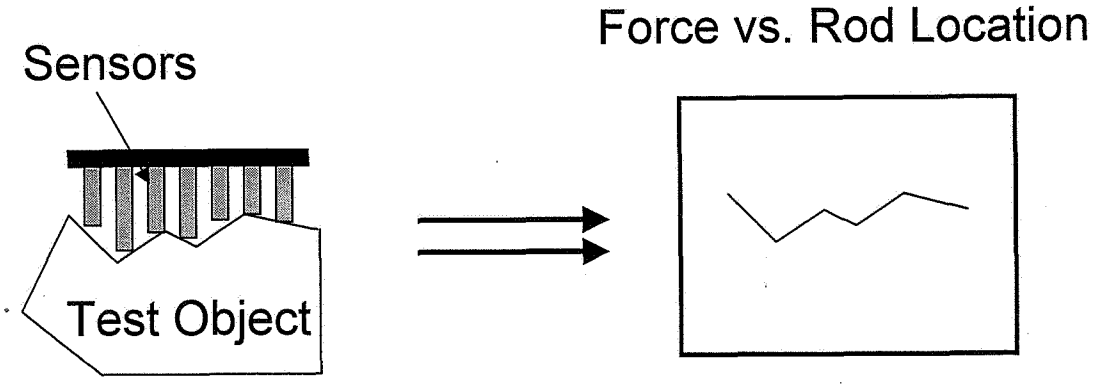

Concept is to have levels of force calculated from change in flux to give a visual map of an object

Galfenol

- Iron & Gallium alloy
- Under stress alloy's permeability changes
- Fe_xGa_x with $15 < x < 28$ giving useful mechanical and transduction characteristics
- Polycrystalline and Single Crystal types
  - Single crystal more costly
  - Polycrystalline has 2 grades:
    - Production grade
    - Research ← slower growth rate so properties are closer to those of the single crystal
    - Research grade used in this experiment

Circuit Design

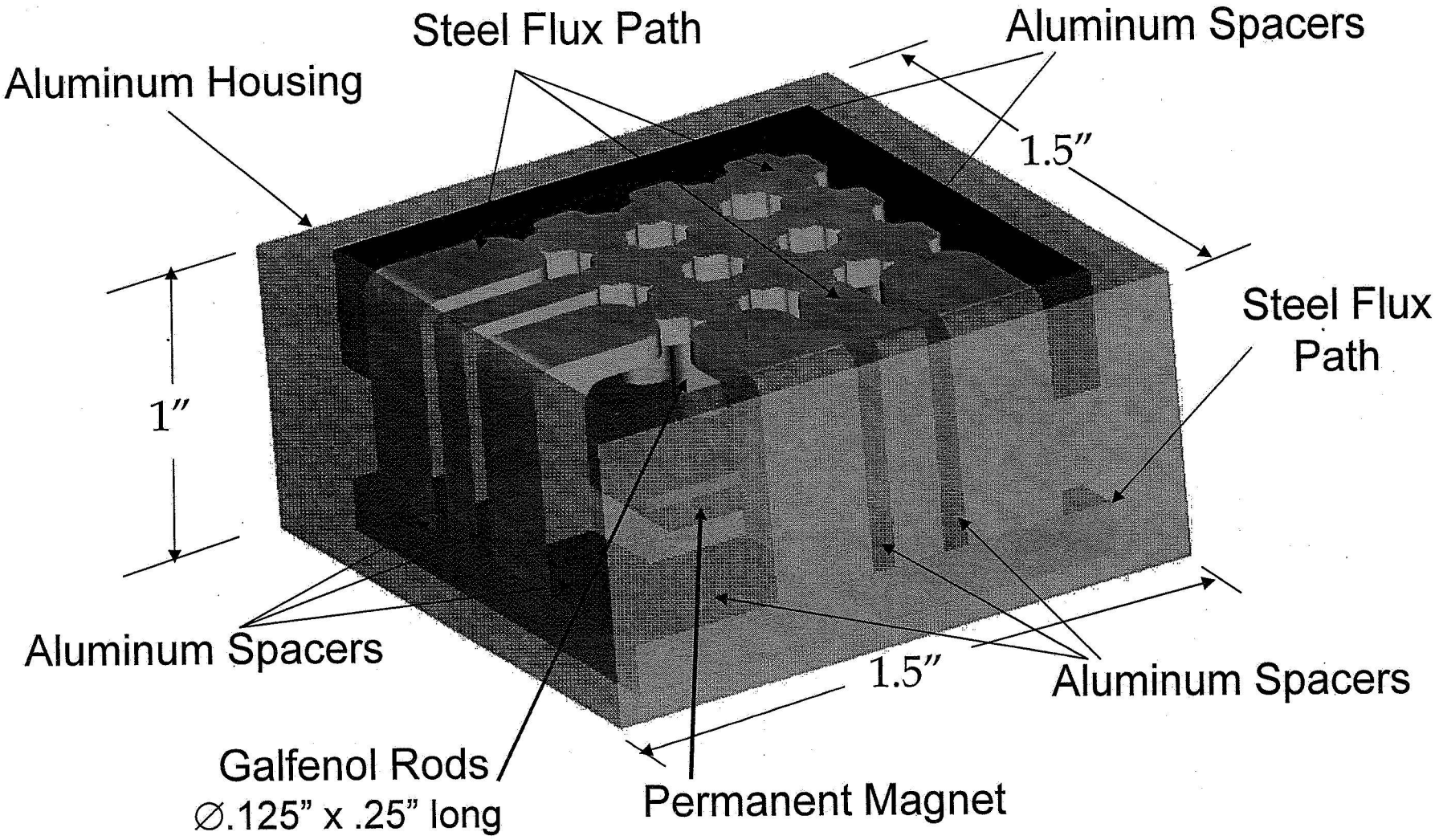

2-D Oersted Magnetic Modeling

Galfenol under no stress

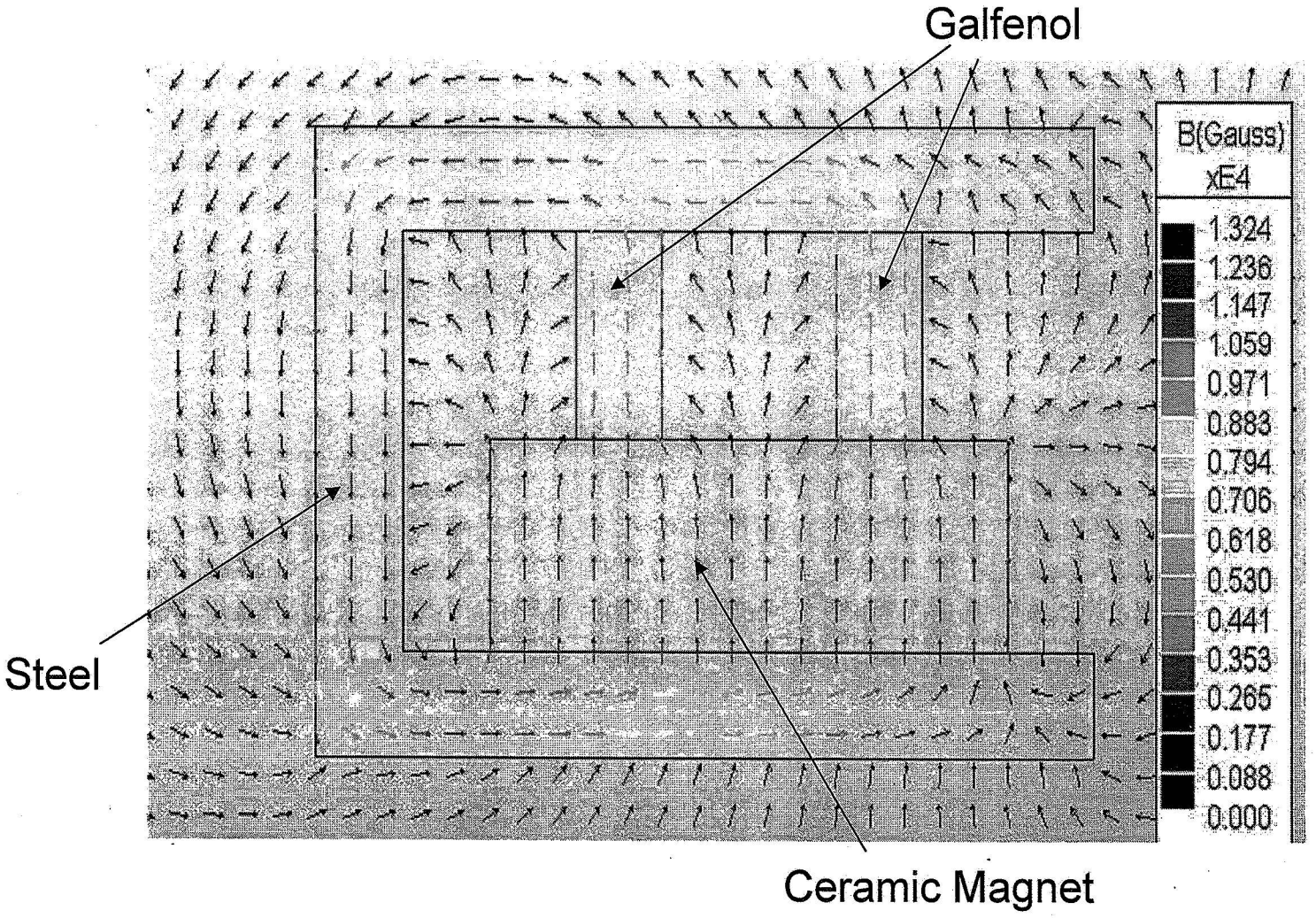

3-D AMPERES Modeling

Galfenol under no stress

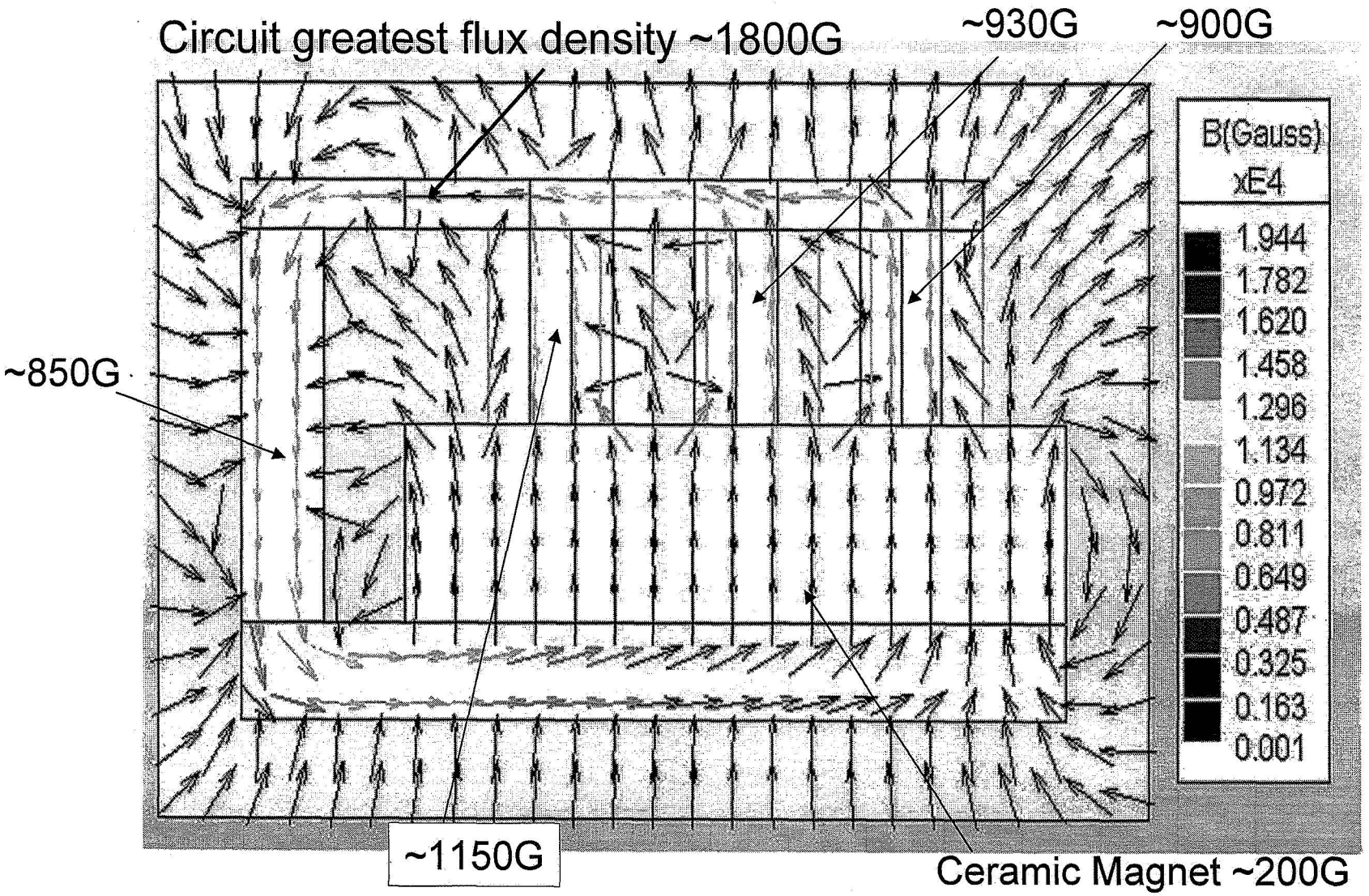

3-D Model Top View

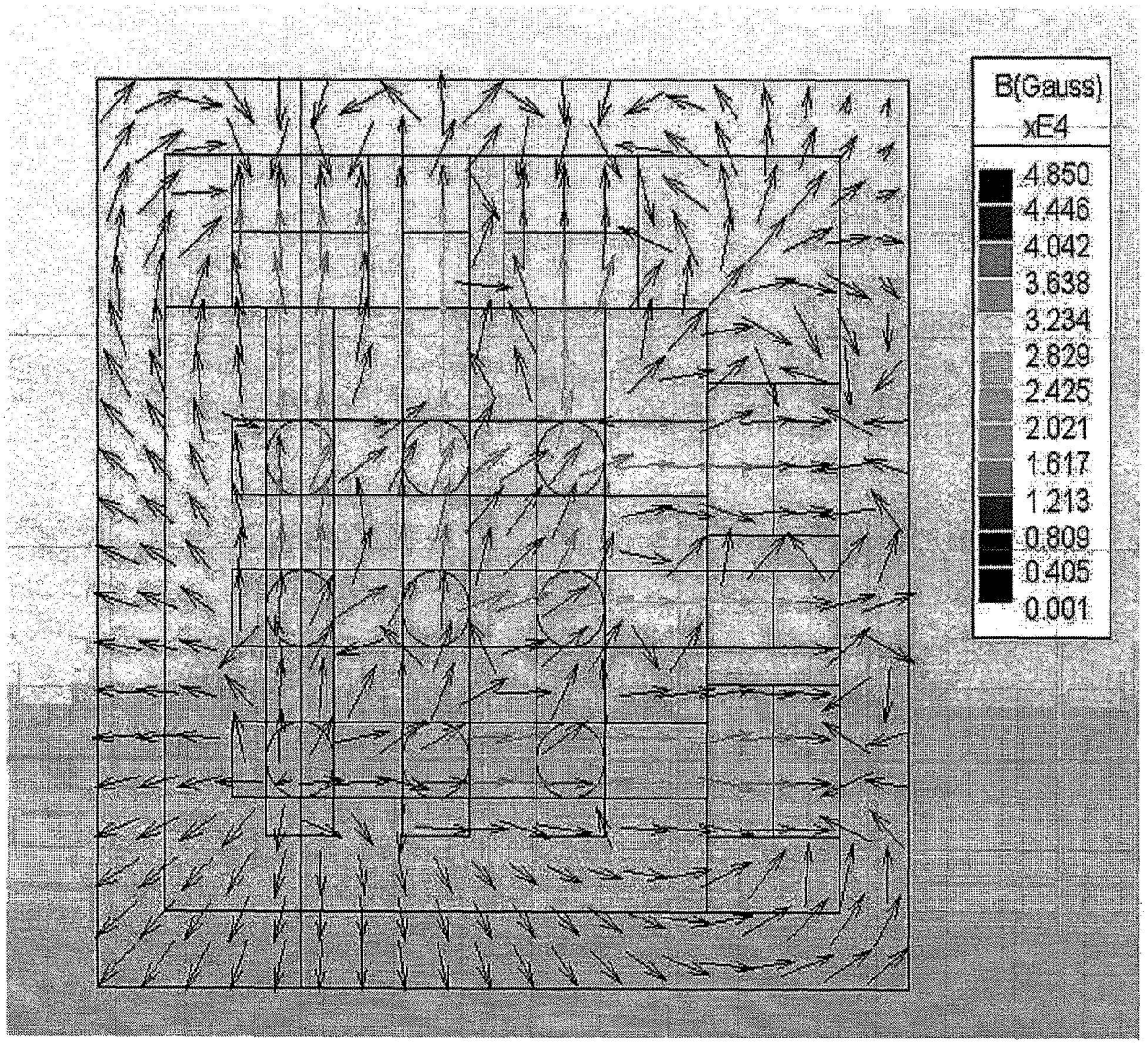

Modeling Results

Location	Stress (MPa)	x(in)	y (in)	z (in)	Bm (Gauss)
Top of Central Rod	0	0.500	0.500	0.625	5651
Side Steel Path #1	0	0.250	1.125	0.688	379
Side Steel Path #2	0	0.500	1.125	0.688	636
Side Steel Path #3	0	0.750	1.125	0.688	295
Side Steel Path #4	0	1.125	0.75	0.6875	276
Side Steel Path #5	0	1.125	0.500	0.688	501
Side Steel Path #6	0	1.125	0.25	0.6875	340
Top of central rod	15	0.500	0.500	0.625	9013
Side Steel Path #1	15	0.250	1.125	0.688	382
Side Steel Path #2	15	0.500	1.125	0.688	641
Side Steel Path #3	15	0.750	1.125	0.688	296
Side Steel Path #4	15	1.125	0.75	0.6875	273
Side Steel Path #5	15	1.125	0.500	0.688	496
Side Steel Path #6	15	1.125	0.25	0.6875	338

- With central rod stressed by 15MPa, only 5 Oersted change in side steel path that corresponds to stressed rod
- Successful indication

Data Acquisition

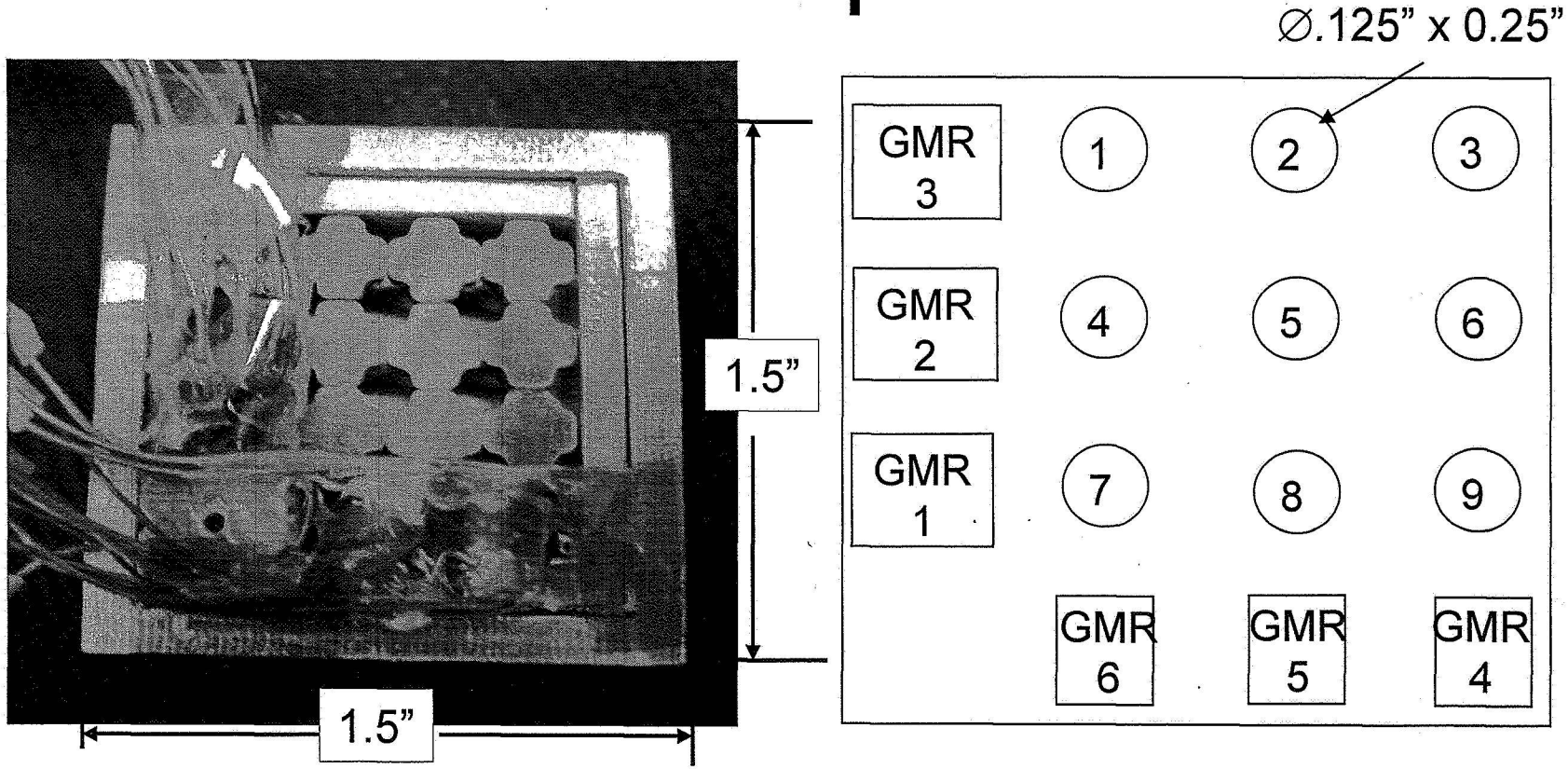

- 6 Giant MagnetoResistive (GMR) sensors, part #AA-005-02; linear range from 10 to 70 Oe and .165 ±0.03 mV/Oe resolution
- Sensors are excited with 3.33 V and a 4 Hz lowpass filter is used to reduce noise.

Static Loading Results

- Used a force gage to load a single rod up to ~13.5 lb
- Results were never repeatable and only one to three rods were indicated correctly for a certain load level that was applied to each rod
- Decided to try dynamic loading

Dynamic Loading

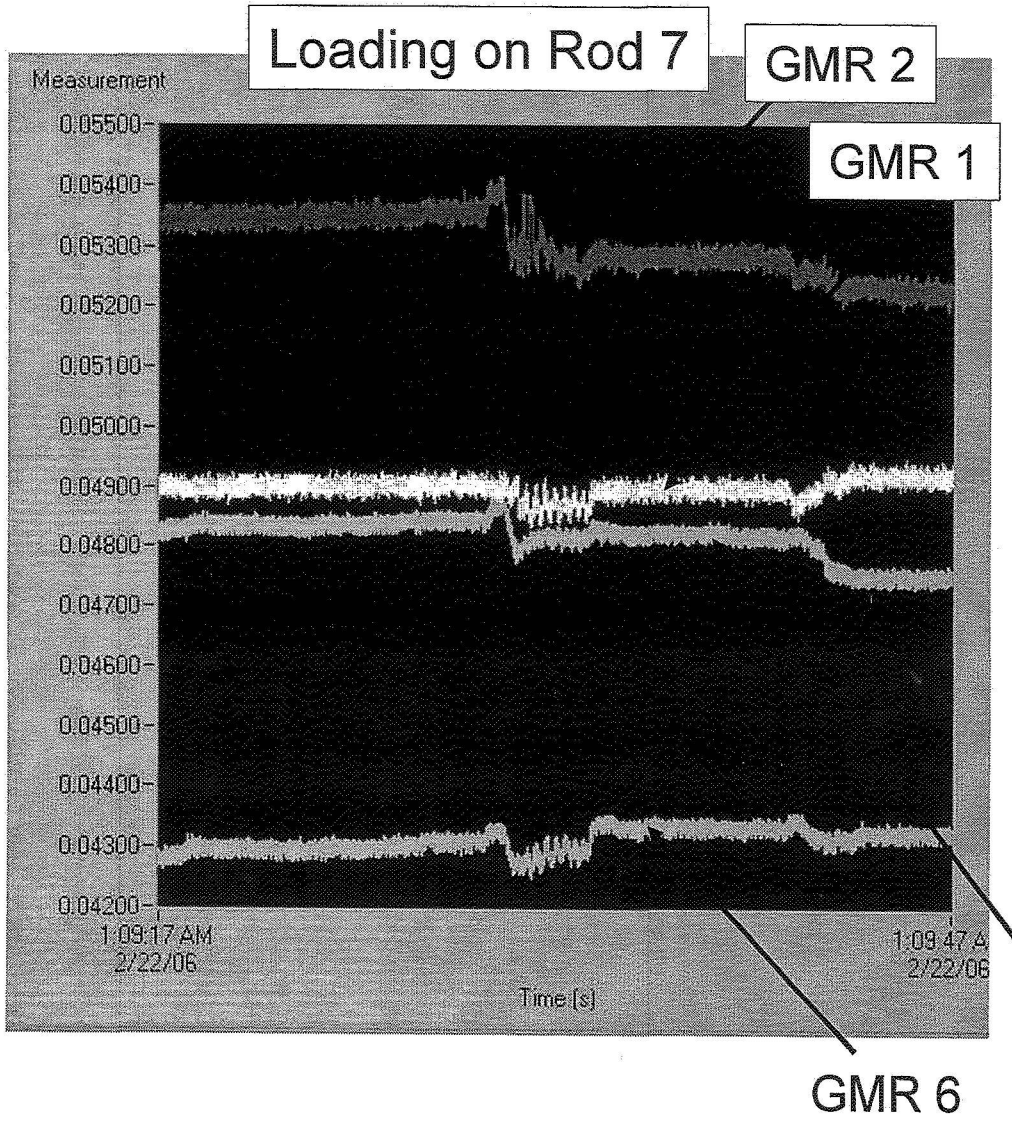

- Decreased circuit to 2 x 2 to simplify readings
- Results were consistent and correct except for rod 7; GMR 1 was not always correctly indicated
  - Error may be in GMR location as GMR 2 is closer to front of steel pathway

Dynamic Results

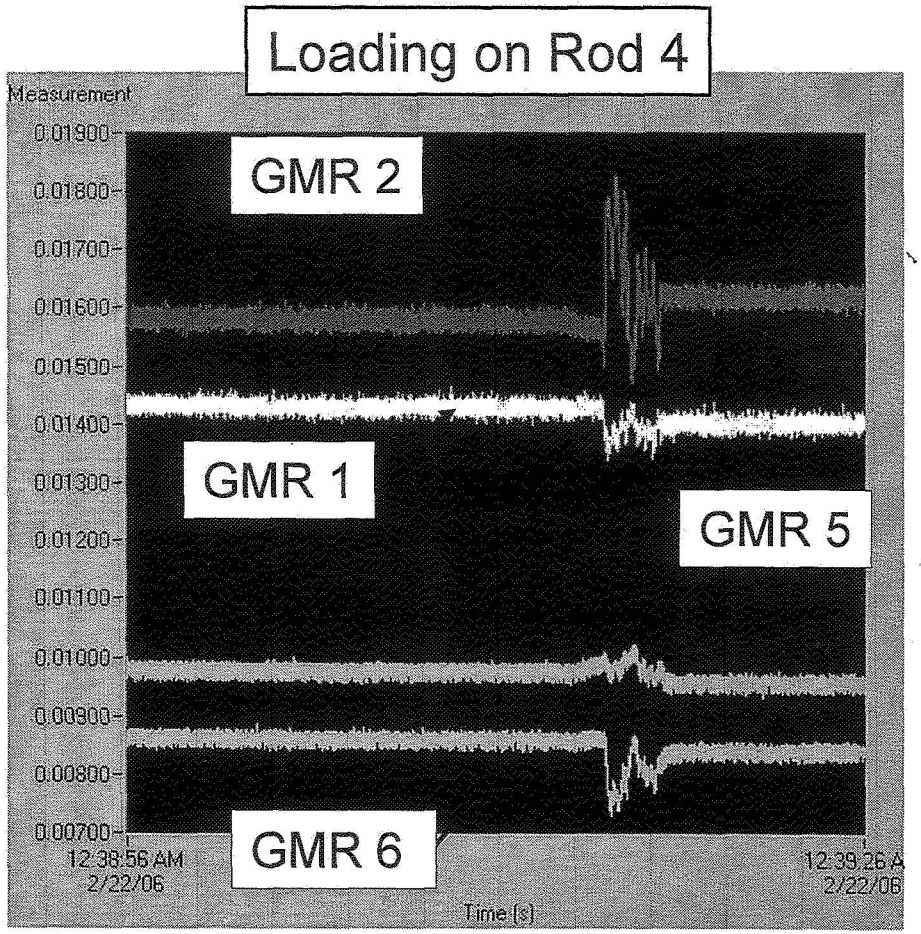

- 2x2 array
- Correct indication in GMRs 2 & 6

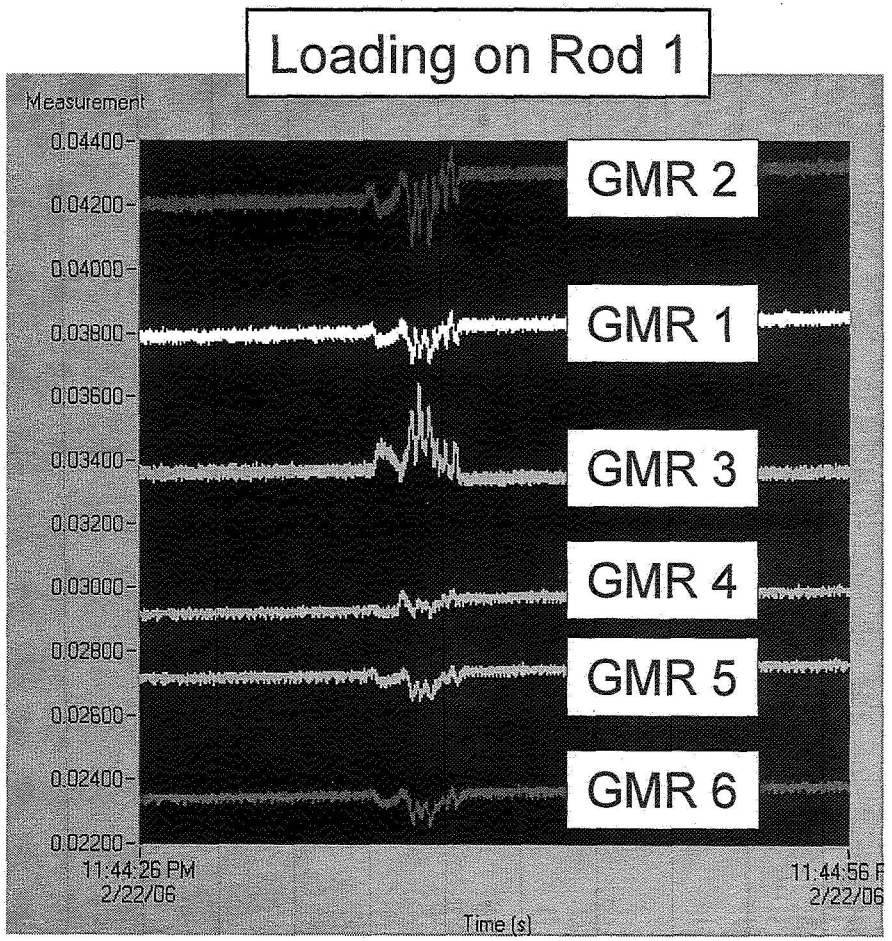

- 3x3 array
- Correct indication on GMR 3, but
- 4-6 are hard to see any differences

Conclusions

- Static loading is complicated and so more investigation and research is required to understand flux travels in the circuit
- Dynamic loading works well in 2x2 array except possibly rod 7
  - GMRs are very sensitive to their distance from the edge of the steel path. GMR 1 is not quite as close as GMR 4 to the edge and so may be why rod 7 is not being indicated correctly each time.
- Dynamic loading results in 3x3 array will improve with use of magnetic grease to fill air gaps

Future Work

- Sense coils will be placed around the Galfenol rods to measure the actual flux change
- Strain gages will be attached to the Galfenol and will be used to ensure a high enough stress is applied to get a measurable change in flux.
- Magnetic grease use with 3x3 array